Temperature-Dependent Proton NMR Investigation of the Electronic Structure of the Trinuclear Iron Cluster of the Oxidized *Desulfovibrio gigas* Ferredoxin II

Anjos L. Macedo, Isabel Moura, and José J. G. Moura*

Centro de Tecnologia Química e Biológica and Universidade Nova de Lisboa, Apartado 127, 2780 Oeiras, Portugal

Jean Le Gall

Department of Biochemistry, University of Georgia, Athens, Georgia 30602

Boi Hanh Huynh*

Department of Physics, Rollins Research Center, Emory University, Atlanta, Georgia 30322

Received May 12, 1992

Proton NMR sprectra of the native (oxidized) *Desulfovibrio gigas* ferredoxin II (a protein which contains only a [3Fe-4S] cluster as its prosthetic group) have been recorded at 300 and 500 MHz. Proton resonances are observed between 6 and 30 ppm, and their temperature dependences are determined over the range 293–308 K. On the basis of the nuclear Overhauser effect and relaxation measurements, the two most downfield-shifted signals (29.0 and 24.4 ppm at 303 K) are assigned to a pair of β-CH_2 protons of one of the cysteinyl residues coordinated to the [3Fe-4S] cluster. Except for these two most downfield shifted signals, which show Curie type temperature dependence, the others show anti-Curie dependence. To analyze the temperature dependence of these resonances a Heisenberg–Dirac–Van Vleck spin-coupling model is introduced. It is found that the observed different types of temperature dependence can be explained by the presence of different exchange coupling interactions between the three iron sites; assuming $J_{13} = J_{23} = J$ and $J_{12} = J + \Delta J$ ($\Delta J > 0$), the β-CH_2 protons of the cysteine ligated to iron site 3 show Curie behavior, while protons of cysteines bound to iron sites 1 and 2 show anti-Curie behavior. Detailed analysis futher suggests that $J \approx 300$ cm^{-1} and that the coupling constants between the iron sites are slightly different: $\Delta J/J \approx 0.02$. Using the available X-ray crystallographic coordinates together with the pattern observed for the two most downfield shifts, we have tentatively assigned them to the methylene protons of Cys 50.

Introduction

Iron–sulfur proteins are a class of proteins with unique prosthetic groups composed of iron and sulfur atoms termed the iron–sulfur centers. These proteins perform diversified enzymatic functional roles besides electron transfer,[1-4] and the iron–sulfur centers constitute a distinct group of molecular entities that are rich in structural, chemical and physical properties.[5-10] Three-dimensional structures of various iron–sulfur centers are available through X-ray crystallographic studies of several prototype iron–sulfur proteins[11-20] and the presence of four basic structures for the iron–sulfur centers are now well established: the FeS_4 center, the [2Fe-2S], the [3Fe-4S], and the [4Fe-4S] clusters. Among these four basic structures, the [3Fe-4S] cluster is the latest entry discovered around 1980.[21,22] Its intriguing structure, a cubane [4Fe-4S] structure lacking a corner iron atom, and the capability of proteins containing the [3Fe-4S] cluster to incorporate an additional iron atom or an atom of other transition metals into the [3Fe-4S] structure transforming the cluster into a [4Fe-4S] cluster or a mixed metal cluster[7,9,23-28] demonstrate the structural versatility of iron–sulfur clusters and have stimulated the dramatic increase of interests in the study of iron–sulfur proteins, as well as model compounds, for the past decade.

* To whom correspondence should be addressed.

(1) Lovenberg, W. *Iron-sulfur Proteins*; Academic Press: New York, 1973–77; Vols. I–III.
(2) Spiro, T. G. *Iron-sulfur Proteins*; John Wiley & Sons: New York, 1982; Vol. IV.
(3) Switzer, R. L. *BioFactors* **1989**, *2*, 77–86.
(4) Beinert, H. *FASEB J.* **1990**, *4*, 2483–2491.
(5) Backes, G.; Mino, Y.; Loehr, T. M.; Meyer, T. E.; Cusanovich, M. A.; Sweeney, W. V.; Adman, E. T.; Sanders-Loehr, J. *J. Am. Chem. Soc.* **1991**, *113*, 2055–2064.
(6) Bertini, I.; Briganti, F.; Luchinat, C.; Scozzafava, A.; Sola, M. *J. Am. Chem. Soc.* **1991**, *113*, 1237–1245.
(7) Holm, R. H.; Ciurli, S.; Weigel, J. A. *Progress in Inorganic Chemistry: Bioinorganic Chemistry*; Lippard, S. J., Ed.; John Wiley & Sons: New York, 1990; Vol. 38, pp 1–74.
(8) Moura, I.; Macedo, A.; Moura, J. J. G. *Advanced EPR and Applications in Biology and Biochemistry*; Hoff, A. J., Ed.; Elsevier: Amsterdam, 1989; pp 813–838.
(9) Stack, T. D. P.; Weigel, J. A.; Holm, R. H. *Inorg. Chem.* **1990**, *29*, 3745–3760.
(10) Backes, G.; Mino, Y.; Loehr, T. M.; Meyer, T. E.; Cusanovich, M. A.; Sweeney, W. V.; Adman, E. T.; Sander-Loehr, J. *J. Am. Chem. Soc.* **1991**, *113*, 2055–2064.
(11) Watenpaugh, K. D.; Sieker, L. C.; Herriott, J. R.; Jensen, L. H. *Acta Crystallogr., Sect. B* **1973**, *B29*, 943–956.
(12) Adman, E.T.; Sieker, L. C.; Jensen, L. H. *J. Biol. Chem.* **1976**, *251*, 3801–3806.
(13) Carter, C. W., Jr.; Kraut, J.; Freer, S. T.; Xuong, Ng. H.; Alden, R. A.; Bartsch, R. G. *J. Biol. Chem.* **1974**, *249*, 4212–4225.
(14) Frey, M.; Sieker, L. C.; Payan, F.; Haser, R.; Bruschi, M.; Pepe, G.; LeGall, J. *J. Mol. Biol.* **1987**, *197*, 525–541.
(15) Fukuyama, K.; Matsubara, H.; Tsukihara, T.; Katsube, Y. *J. Mol. Biol.* **1989**, *210*, 383–398.
(16) Stout, C. D. *J. Mol. Biol.* **1989**, *205*, 545–555.
(17) Stout, G. H.; Turley, S.; Sieker, L. C.; Jensen, L. H. *Proc. Natl. Acad. Sci. U.S.A.* **1988**, *85*, 1020–1022.
(18) Kissinger, C. R.; Adman, E. T.; Sieker, L. C.; Jensen, L. H.; LeGall, J. *FEBS Lett.* **1989**, *244*, 447–450.
(19) Kissinger, C. R.; Adman, E. T.; Sieker, L. C.; Jensen, L. H. *J. Am. Chem. Soc.* **1988**, *110*, 8721–8723.
(20) Fukuyama, K.; Hase, T.; Matsumoto, S.; Tsukihara, T.; Katsube, Y.; Tanaka, N.; Kakudo, M.; Wada, K.; Matsubara, H. *Nature* **1980**, *286*, 522–524.
(21) Emptage, M. H.; Kent, T. A.; Huynh, B. H.; Rawlings, J.; Orme-Johnson, W. H.; Münck, E. *J. Biol. Chem.* **1980**, *255*, 1793–1796.
(22) Huynh, B. H.; Moura, J. J. G.; Moura, I.; Kent, T. A.; LeGall, J.; Xavier, A. V.; Münck, E. *J. Biol. Chem.* **1980**, *255*, 3242–3244.

0020-1669/93/1332-1101$04.00/0

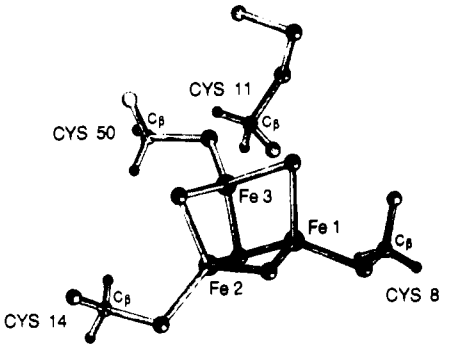

Figure 1. Three dimensional structure of the [3Fe-4S] cluster in *D. gigas* Fd II. The structure is derived from the crystallographically determined X-ray coordinates provided by Dr. L. C. Sieker (personal communication). This figure indicates the geometrical arrangement of the iron and labile sulfur atoms at the core as well as the cysteinyl ligands. Also shown are the β-CH_2 protons and the methanethiol group of the modified Cys 11.

Ferredoxin II (Fd II) isolated from *Desulfovibrio* (*D.*) *gigas* is a tetramer composed of four identical subunits. Each subunit is composed of 58 amino acids, including 6 cysteine residues. It has a molecular mass of 6 kDa and contains a single [3Fe-4S] cluster.[29] Crystallographic X-ray structural analysis[18,19] indicates that the cluster is bound to the polypeptide chain by three cysteinyl residues: Cys 8, Cys 14 and Cys 50. The residue Cys 11 (a potential forth ligand if the cluster were a [4Fe-4S] cluster) is not bound and tilted toward the solvent away from the cluster (Figure 1). An unexpected observation from the X-ray data is that Cys 11 appears to be chemically modified, possibly a methanethiol group.[18] It is currently undetermined whether this chemical modification is present in the native protein or a result of the crystallization process. The other two cysteines, Cys 18 and Cys 42, form a disulfide bridge.

A major portion of our current understanding concerning the physical and biochemical properties of [3Fe-4S] clusters is derived from investigations performed on *D. gigas* Fd II.[30,31] Other [3Fe-4S] cluster-containing proteins subjected to extensive investigations are the beef heart aconitase,[4,32,33] the *Azotobacter vinelandii* Fd I,[16,17,22,34,35] the *D. gigas* [NiFe] hydrogenase,[36] the *Escherichia coli* fumarate reductase,[37] and succinate dehydrogenase.[38] In all the above mentioned proteins, the [3Fe-4S] cluster can be stabilized in two oxidation states: $[3Fe\text{-}4S]^{1+}$ and $[3Fe\text{-}4S]^{0}$. Further reduction of the cluster into a formal $[3Fe\text{-}4S]^{2-}$ oxidation state has been suggested by a cyclic voltammetry study of *D. africanus* Fd III.[39] Unfortunately, this putative three-electron reduced species can not be generated in bulk quantity, preventing spectroscopic characterization.

In the oxidized $[3Fe\text{-}4S]^{1+}$ cluster, the iron atoms are high-spin ferric ($S = {}^5/_2$) and are antiferromagnetically coupled, forming a ground electronic state with a system spin of ${}^1/_2$. A saturation magnetization study on *D. gigas* Fd II[40] establishes a lower limit of 200 cm^{-1} for the exchange coupling interaction within the $[3Fe\text{-}4S]^{1+}$ cluster. For the reduced $[3Fe\text{-}4S]^{0}$ cluster, Mössbauer investigations[20,21,23,29] indicate that the additional electron is shared by two iron sites resulting in a delocalized pair $[2Fe^{2.5+}]$ and a high-spin ferric site. A low-temperature magnetic circular dichroism study of reduced *D. gigas* Fd II[41] suggests that the electronic ground state of the reduced cluster has a system spin of 2. Detailed analysis of the Mössbauer data[30] reveals a spin of ${}^9/_2$ for the delocalized iron pair, which is antiferromagnetically coupled to the ferric ion ($S = {}^5/_2$) resulting in the system spin of 2. On the basis of these studies, a double exchange interaction, in addition to the more conventional Heisenberg exchange interaction, was introduced to rationalize the observed electron delocalization and the ferromagnetic nature of the delocalized iron pair, as indicated by their spin value of ${}^9/_2$.[30,31] Subsequent theoretical investigations[42] further suggest that double exchange interaction can be used to explain the electronic and hyperfine properties of the [4Fe-4S] cluster, including many "abnormalities" recently observed for the reduced $[4Fe\text{-}4S]^{1+}$ cluster, such as the coexistence of multiple electronic ground states with different spin quantum numbers.[43-45]

It has been recognized for quite some time that proton NMR spectroscopy is a sensitive tool for probing the electronic properties of proteins containing paramagnetic centers.[46] In the case that the paramagnetic center is a polynuclear metal cluster, proton NMR spectroscopy not only can yield information concerning the whole cluster, such as the system spin and energy level distribution, the method can also provide information regarding each individual metal atom, such as the orientation of the intrinsic spin of each atom and the magnitudes of the exchange coupling interactions between the metal atoms.[47,48] Early proton NMR investigations of [2Fe-2S] cluster containing proteins[49,50] have established the antiferromagnetic coupling nature of the [2Fe-2S] cluster and have determined the exchange coupling constants for both the oxidized and reduced states of the [2Fe-2S] cluster. More recently, the method has been applied to the study of proteins containing [4Fe-4S] clusters,[51-54] and detailed information has

(23) Moura, J. J. G.; Moura, I.; Kent, T. A.; Lipscomb, J. D.; Huynh, B. H.; LeGall, J.; Xavier, A. V.; Münck, E. *J. Biol. Chem.* **1982**, *257*, 6259–6267.
(24) Kent, T. A.; Dreyer, J.-L.; Kennedy, M. C.; Huynh, B. H.; Emptage, M. H.; Beinert, H.; Münck, E. *Proc. Natl. Acad. Sci. U.S.A.* **1982**, *79*, 1096–1100.
(25) George, S. J.; Armstrong, F. A.; Hatchikian, E. C.; Thomson, A. J. *Biochem. J.* **1989**, *264*, 275–284.
(26) Moura, I.; Moura, J. J. G.; Münck, E.; Papaefthymiou, V.; LeGall, J. *J. Am. Chem. Soc.* **1986**, *108*, 349–451.
(27) Surerus, K.;, Münck, E.; Moura, I.; Moura, J. J. G.; LeGall, J. *J. Am. Chem. Soc.* **1987**, *109*, 3805–3807.
(28) Conover, R. C.; Park, J.-B.; Adams, M. W. W.; Johson, M. K. *J. Am. Chem. Soc.* **1990**, *112*, 4562–4564.
(29) Xavier, A. V.; Moura, J. J. G.; Moura, I. *Struct. Bonding* **1981**, *43*, 187–213.
(30) Papaefthyniou, V.; Girerd, J.-J.; Moura, I.; Moura, J. J. G.; Münck, E. *J. Am. Chem. Soc.* **1987**, *109*, 4703–4710.
(31) Münck, E.; Papaefthymiou, V.; Surerus, K. K.; Girerd, J.-J. *Metal Clusters in Proteins*; Que, L., Ed.; ACS Symposium Series 372; American Chemical Society: Washington, DC, 1988; pp 302–325.
(32) Emptage, M. H. *Metal Clusters in Proteins*; Que, L., Ed.; ACS Symposium Series 372; American Chemical Society: Washington, DC, 1988; pp 343–371.
(33) Plank, D. W.; Kennedy, M. C.; Beinert, H.; Howard, B. *J. Biol. Chem.* **1989**, *264*, 20385–20393.
(34) Beinert, H.; Thomson, A. J. *Arch. Biochem. Biophys.* **1983**, *222*, 333–361.
(35) Thomson, A. J. *FEBS Lett.* **1991**, *285*, 230–236.
(36) Teixeira, M.; Moura, I.; Xavier, A. V.; Moura, J. J. G.; LeGall, J.; DerVartanian, D. V.; Peck, H. D., Jr.; Huynh, B. H. *J. Biol. Chem.* **1989**, *264*, 16435–16450.
(37) (a) Werth, M. T.; Cecchini, G.; Manodori, A.; Ackrell, B. A. C.; Schöder, I.; Gunsalus, R. P.; Johnson, M. K. *Proc. Natl. Acad. Sci. U.S.A.* **1990**, *87*, 8965–8969. (b) Morningstar, J. E.; Johnson, M. K.; Cecchini, G.; Ackrell, B. A. C.; Kearney, E. B. *J. Biol. Chem.* **1985**, *260*, 13631–13638.
(38) Ohnishi, T. *Curr. Top. Bioenerg.* **1987**, *15*, 37–65.
(39) Armstrong, F. A.; Butt, J. N.; George, S. J.; Hatchikian, E. C.; Thomson, A. J. *FEBS Lett.* **1989**, *259*, 15–18.
(40) Day, E. P.; Peterson, J.; Bonvoisin, J. J.; Moura, I.; Moura, J. J. G. *J. Biol. Chem.* **1988**, *263*, 3684–3689.
(41) Thomson, A. J.; Robinson, A. E.; Johnson, M. K.; Moura, J. J. G.; Moura, I.; Xavier, A. V.; LeGall, J. *Biochim. Biophys. Acta* **1981**, *670*, 93–100.
(42) (a) Noodleman, L. *Inorg. Chem.* **1991**, *30*, 246–256. (b) *Ibid*, 256–264.
(43) Carney, M. J.; Papaefthymiou, G. C.; Whitener, M. A.; Spartalian, K.; Frankel, R. B.; Holm, R. H. *Inorg. Chem.* **1988**, *27*, 346–352.
(44) Auric, P.; Gaillard, J.; Meyer, J.; Moulis, J.-M. *Biochem. J.* **1987**, *242*, 525–530.
(45) Gaillard, J.; Moulis, J.-M.; Auric, P.; Meyer, J. *Biochemistry* **1986**, *25*, 464–468.
(46) La Mar, G. N., Horrocks, W. D., Jr., Holm, R. H., Eds.; *NMR of Paramagnetic Molecules*; Academic Press: New York, 1973.
(47) Banci, L.; Bertini, I.; Briganti, F. *New J. Chem.* **1991**, *15*, 467–477.
(48) Banci, L.; Bertini, I.; Luchinat, C. *Struct. Bonding* **1990**, *72*, 113–136.
(49) Salmeen, I.; Palmer, G. *Arch. Biochem. Biophys.* **1972**, *150*, 767–773.
(50) Dunham, W. R.; Palmer, G.; Sands, R. H.; Bearden, A. J. *Biochim. Biophys. Acta* **1971**, *253*, 373–384.
(51) Bertini, I.; Briganti, F.; Luchinat, C.; Scozzafava, A.; Sola, M. *J. Am. Chem. Soc.* **1991**, *113*, 1237–1245.
(52) Banci, L.; Bertini, I.; Briganti, F.; Scozzafava, A.; Oliver, M. V. *Inorg. Chim. Acta* **1991**, *180*, 171–175.

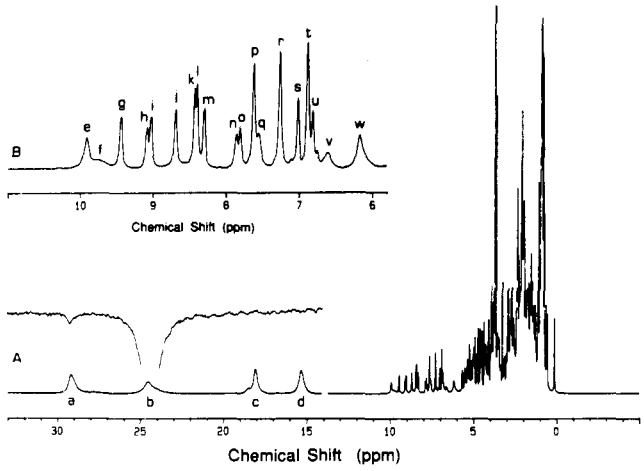

Figure 2. Proton NMR spectra of native (oxidized) *D. gigas* Fd II. The spectra were recorded at 303 K with experimental conditions described in the Material and Methods section. Resonances are labeled from *a* to *w* starting from the low-field region. The complete spectrum is shown in (A). The low-field region has been expanded 6 times in height. Details of the aromatic spectral region (high-field region) is shown in (B). The 1D NOE spectrum obtained by irradiation at resonance *b* is shown in (C).

been obtained concerning the electronic and magnetic properties of the cluster.

In this manuscript, a proton NMR study of the oxidized *D. gigas* Fd II is reported. A theoretical model based on the Heisenberg exchange coupling scheme is used to analyze the temperature dependences of the observed contact shifts of the C_β methylene protons of the cysteine residues coordinated to the [3Fe-4S] cluster.

Materials and Methods

D. gigas Fd II was purified as previously described[55] with a slight modification. The last purification step was performed in a gel filtration column (TSK-G3000 SW) by HPLC and the elution buffer was 0.5 M Tris-HCl at pH 7.6. The NMR samples (1 mM) were concentrated and exchanged with phosphate buffer (0.1 M, pH 7.6) and D_2O (99.9%) in AMICON centricons with cut off at 10 kDa.

The proton NMR experiments were carried out either in a 300 MHz or a 500 MHz Fourier transform Bruker AMX spectrometer equipped with a temperature control unit. The proton nuclear Overhauser effect (NOE) experiments were performed at the 300 MHz spectrometer using the super-WEFT pulse sequence (180–τ–90–AQ)[56] with recycle times and τ values of approximately 100 ms, providing water suppression. Selective saturation of the resonance at about 25 ppm was made during the delay time τ. Difference spectra were obtained by subtracting the off resonance spectra from the on resonance spectra as described in ref 51. T_1 measurements were made using the inversion–recovery sequence.

Results

A 500 MHz ^{1}H NMR spectrum of oxidized Fd II from *Desulfovibrio gigas* is shown in Figure 2 (spectrum *A*). The data were recorded at 303 K. Isotropically shifted resonances (labeled *a*–*w*) are detected in the 30–6 ppm region. The temperature dependences of these resonances are plotted in Figure 3. Except for the peaks *a* (at 29.0 ppm) and *b* (at 24.4 ppm) which show temperature dependence of the Curie type, the others exhibit anti-Curie type dependence. A detailed study on the assignments and T_1 measurements of these resonances will be the subject of a separate publication, and in this report, the focus is on the well shifted downfield resonances (peaks *a*–*d*). Their large downfield shifts indicate that they are most likely originating from protons

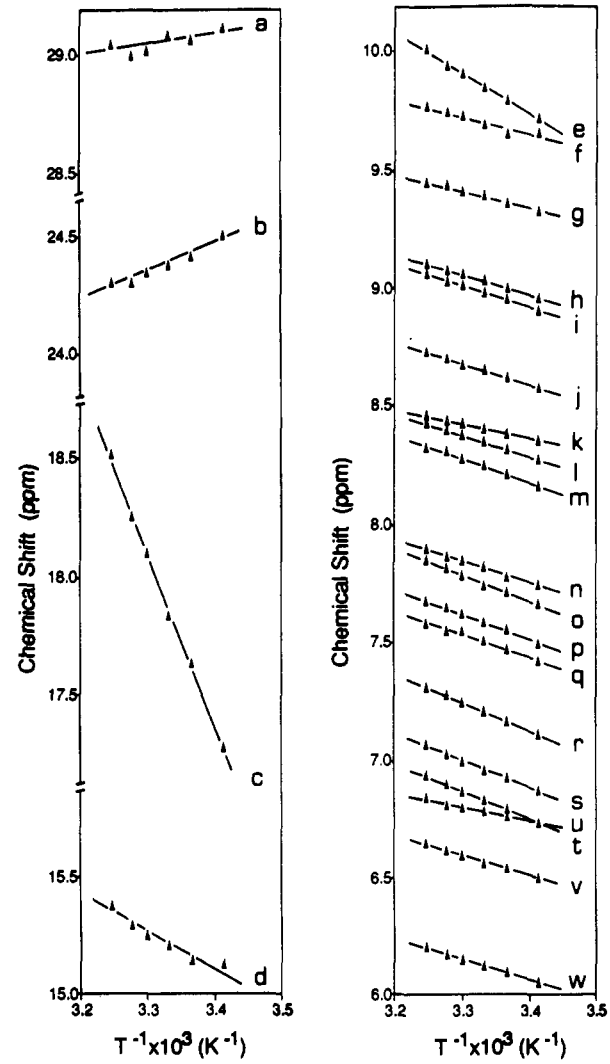

Figure 3. Experimental temperature dependence of the observed proton NMR resonances of oxidized *D. gigas* Fd II. The resonances are detected between 6 and 30 ppm and are labeled as in Figure 2. The solid lines indicates the trends of their temperature dependence and are not fits of the experimental data.

of the cysteine residues coordinated to the [3Fe-4S] cluster. The observed different types of temperature dependence for these resonances are indicative of the presence of a nearby paramagnetic spin-coupled iron cluster and reflect the intrinsic spin orientations of the iron atoms (to which the cysteine residues are coordinated) with respect to the system spin of the cluster.[47-53,57] A spin-coupling model for the oxidized [3Fe-4S] cluster presented in the following section indicates that only the protons of a cysteine coordinated to one particular iron site exhibit Curie type temperature dependent contact shifts. Consequently, peaks *a* and *b* are attributed to the β-CH_2 protons of a same cysteine residue. Further evidence in support of this assignment is obtained from 1D ^{1}H NOE and T_1 measurements. A difference spectrum between spectra recorded without and with saturation of signal *b* is shown in Figure 2 (spectrum C). A weak, but definitive, NOE is detected at signal *a*, in support of the geminal nature of these two resonances. The T_1's measured for peaks *a*, *b*, *c*, and *d* are 4.3, 3.1, 4.0 and 7.0 ms, respectively. These relatively short T_1's are characteristic for the β-CH_2 protons of cysteine coordinated to a paramagnetic metal center.[51,54,57,58] Proton NOE has also been observed between two most downfield shifted resonances of *A. vinelandii* Fd I,[54] which contains both a [3Fe-

(53) Bertini, I.; Briganti, F.; Luchinat, C.; Scozzafava, A. *Inorg. Chem.* **1990**, *29*, 1874–1880.
(54) Cheng, H.; Grohmann, K.; Sweeney, W. *J. Biol. Chem.* **1990**, *265*, 12388–12392.
(55) Bruschi, M.; Hatchikian, C. E.; LeGall, J.; Moura, J. J. G.; Xavier, A. V. *Biochim. Biophys. Acta* **1976**, *449*, 275–284.
(56) Inubushi, T.; Becker, E. D.; *J. Magn. Reson.* **1983**, *51*, 128–133.
(57) Dugad, L. B.; La Mar, G. N.; Banci, L.; Bertini, I. *Biochemistry* **1990**, *29*, 2263–2271.
(58) Busse, S. C.; La Mar, G. N.; Howard, J. B. *J. Biol. Chem.* **1991**, *266*, 23714–23723.

4S] and a [4Fe-4S] cluster. These downfield resonances were assigned to the geminal β-CH_2 cysteinyl protons bound to the [3Fe-4S] cluster.[54] Our current results strongly support this assignment.

Theoretical Considerations

In order to gain information concerning the electronic structure of and the exchange interactions within the [3Fe-4S] cluster in oxidized Fd II, we apply a spin-coupling model introduced by Kent et al.[59] to calculate the energy level scheme of the cluster, and we employ a theory developed by Bertini et al.[51] to estimate the contact shifts of the coordinated cysteine protons. On the basis of the Mössbauer and electron paramagnetic resonance data, Kent et al.[59] had shown that the electronic structure of the oxidized [3Fe-4S] cluster can be characterized as a system containing three exchange-coupled high-spin ferric ions ($S = {}^5/_2$) with the exchange interaction described by the following Heisenberg–Dirac–Van Vleck spin Hamiltonian,

$$\mathcal{H} = J_{12}\mathbf{S}_1\cdot\mathbf{S}_2 + J_{13}\mathbf{S}_1\cdot\mathbf{S}_3 + J_{23}\mathbf{S}_2\cdot\mathbf{S}_3 \quad (1)$$

where $S_1 = S_2 = S_3 = {}^5/_2$ are the intrinsic spin numbers of the ferric ions, and J_{ij} is the exchange coupling constant between the ith and the jth iron sites. From the Mössbauer data,[22,59] it was deduced that $J_{12} > J_{13} \approx J_{23} > 0$. To simplify the data analysis, we assume that $J_{13} = J_{23} = J$ and rewrite $J_{12} = J + \Delta J$. Equation 1 can then be rewritten as

$$\mathcal{H} = J(\mathbf{S}_1\cdot\mathbf{S}_2 + \mathbf{S}_1\cdot\mathbf{S}_3 + \mathbf{S}_2\cdot\mathbf{S}_3) + \Delta J(\mathbf{S}_1\cdot\mathbf{S}_2) \quad (2)$$

and analytical solutions can be readily obtained. The eigenvalue of the nth spin multiplets resulting from eq 2 are given by the simple formula

$$E^n(S_{12}{}^n, S^n) = (J/2)[S^n(S^n+1)] + (\Delta J/2)[S_{12}{}^n(S_{12}{}^n+1)] \quad (3)$$

where $\mathbf{S}^n = \mathbf{S}_1 + \mathbf{S}_2 + \mathbf{S}_3$ is the total spin of the cluster, $\mathbf{S}_{12}{}^n = \mathbf{S}_1 + \mathbf{S}_2$ is the coupled spin of iron sites 1 and 2, and the superscript n indicates the nth spin multiplet level. On the basis of Mössbauer and EPR data, the ground state of the oxidized [3Fe-4S] cluster is described by $S^0 = {}^1/_2$ and $S_{12}{}^0 = 2$.[59] With the energies given by eq 3, the contact shifts of the protons of the cysteine residue coordinated to the ith iron site can be calculated,[47,48]

$$\delta = \left(\frac{2\pi g\beta}{h\gamma(3kT)}\right) \times A_i\left(\frac{\sum_n C_i{}^n S^n(S^n+1)(2S^n+1)\exp(-E^n/kT)}{\sum_n (2S^n+1)\exp(-E^n/kT)}\right) \quad (4)$$

where A_i is the intrinsic isotropic hyperfine coupling constant between the β-CH_2 protons and the coordinated iron site, and can be estimated from the NMR data of monometallic complexes, such as rubredoxin. In our analysis, $A_1 = A_2 = A_3 = 1$ MHz. This value has been used to explain the proton NMR data of the [2Fe-2S] cluster[49,50] and of the [4Fe-4S] clusters,[51,53] and yields a shift of 210 ppm for a reduced monomeric FeS_4 center at 300 K, consistent with experimental data detected for rubredoxin and model compounds.[60] The coefficient $C_i{}^n$ is the ratio of the projections of S_i and S^n along the direction of the magnetic field, and can be calculated using the Wigner–Eckart theorem,[61,62]

$$C_1{}^n = \{[S^n(S^n+1) + S_{12}{}^n(S_{12}{}^n+1) - S_3(S_3+1)][S_{12}{}^n(S_{12}{}^n+1) + S_1(S_1+1) - S_2(S_2+1)]\}/\{[2S^n(S^n+1)][2S_{12}{}^n(S_{12}+1)]\} \quad (5)$$

$$C_2{}^n = \{[S^n(S^n+1) + S_{12}{}^n(S_{12}{}^n+1) - S_3(S_3+1)][S_{12}{}^n(S_{12}{}^n+1) + S_2(S_2+1) - S_1(S_1+1)]\}/\{[2S^n(S^n+1)][2S_{12}{}^n(S_{12}{}^n+1)]\} \quad (6)$$

$$C_3{}^n = [S^n(S^n+1) + S_3(S_3+1) - S_{12}{}^n(S_{12}{}^n+1)]/[2S^n(S^n+1)] \quad (7)$$

Since $S_1 = S_2 = {}^5/_2$, eqs 5 and 6 indicate that $C_1{}^n = C_2{}^n$, as expected for this theoretical approach. Applying eqs 4–7, the temperature dependence of the contact shifts of the β-CH_2 protons can be estimated and the adjustable parameters are only two, namely, J and ΔJ.

Discussion

With the above described theory, the temperature dependences of the ^{1}H NMR shifts of the oxidized [3Fe-4S] cluster in *D. gigas* Fd II can be explained and provide detailed information concerning the exchange coupling interaction within the iron cluster. Assuming $\Delta J = 0$ (i.e., $J_{12} = J_{13} = J_{23}$), all three iron sites are indistinguishable, and at the temperature range of the NMR measurements (293–308 K), only anti-Curie type temperature dependence is expected. The observation of both Curie type and anti-Curie type dependences, therefore, indicates that $\Delta J \neq 0$. With $\Delta J > 0$, iron site 3 becomes inequivalent from the other two sites. Curie type temperature dependence is predicted for the β-CH_2 protons coordinated to iron site 3, while anti-Curie dependence is predicted for the protons coordinated to the other two sites. The rates of the temperature dependences are strongly dependent on the value of ΔJ. Also, since the energies of the spin multiplets are determined by the value of J and the NMR shifts are the result of thermal average over these energy levels, the observed proton NMR shifts are good measurements for J. To determine the approximate values for J and ΔJ, we selected peaks *a* and *b* for the final analysis. This selection was made because peaks *a* and *b* show Curie behavior and can be uniquely assigned to the β-CH_2 protons of the cysteine coordinated to iron site 3. We then performed a search through the parameter space of ΔJ and J and compared the calculated temperature dependence of the proton isotropic shifts with the experimental data. We found that with $J = 300$ cm^{-1} and $\Delta J/J = 0.02$ the estimated contact shifts, 26.8 ppm, for the methylene protons coordinated to iron site 3 at 3.2×10^{-3} K^{-1} agrees very well with the average of the experimental values of peaks *a* and *b*, and the calculated rate of temperature dependence ($+0.7 \times 10^3$ ppm K) parallels the average rate for peaks *a* and *b* ($+0.8 \times 10^3$ ppm K). The proton shifts with anti-Curie dependence are estimated to be smaller and fall in the range of those values observed for peaks *c* and *d*. In order to show the strong dependence of the proton NMR shifts on the parameters ΔJ and J, we plot in Figure 4 the calculated temperature dependence of the proton shifts with the following two sets of parameter values: (1) J value fixed at 300 cm^{-1} and varying $\Delta J/J$ ($\Delta J/J = 0$, 0.02, and 0.05) and, (2) $\Delta J/J$ fixed at 0.02 and varying J value ($J = 250$ cm^{-1}, 300 cm^{-1}, and 350 cm^{-1}). With the J value fixed at 300 cm^{-1}, a variation of $\Delta J/J$ from 0.02 to 0.05 increases the rate of the Curie dependence by more than 4 folds at the experimental temperature range (Figure 4, panel A). With a fixed value of $\Delta J/J$ at 0.02, a variation of the J value by 50 cm^{-1} corresponding to a change of $\sim$5 ppm in shifts (Figure 4, panel B).

The electronic properties of the oxidized [3Fe-4S] cluster has been thoroughly examined through Mössbauer and EPR studies and detailed information for its ground electronic state has been

(59) Kent, T. A.; Huynh, B. H.; Münck, E. *Proc. Natl. Acad. Sci. U.S.A.* **1980**, *77*, 6574–6576.
(60) Werth, M. T.; Kurtz, D. M., Jr.; Moura, I.; LeGall, J. *J. Am. Chem. Soc.* **1987**, *109*, 273–275.
(61) Noodleman, L. *Inorg. Chem.* **1988**, *27*, 3677–3679.
(62) Middleton, P.; Dickson, D. P. E.; Johnson, C. E.; Rush, J. D. *Eur. J. Biochem.* **1980**, *104*, 289–296.

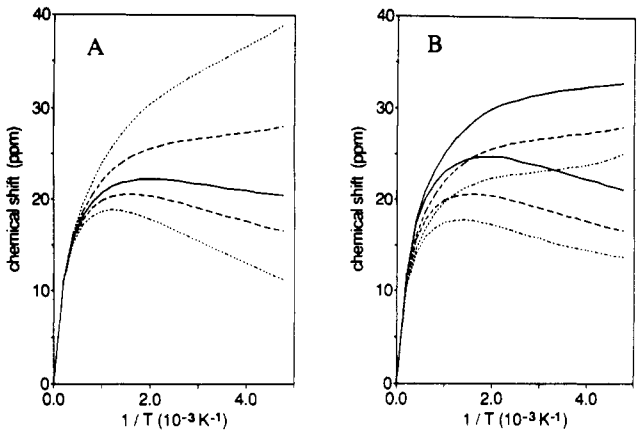

Figure 4. Theoretical temperature dependence of the isotropically contact shifted resonances of the β-CH_2 protons coordinated to the [3Fe-4S] cluster in oxidized *D. gigas* Fd II. Panel A: J value fixed at 300 cm^{-1}, $\Delta J/J = 0$ (solid line); $\Delta J/J = 0.02$ (dashed lines); $\Delta J/J = 0.05$ (dotted lines). Panel B: $\Delta J/J$ value fixed at 0.02, $J = 250$ cm^{-1} (solid lines); $J = 300$ cm^{-1} (dashed lines); $J = 350$ cm^{-1} (dotted lines).

obtained.[20,21,59] The relative strengths of the exchange coupling interactions were deduced from these studies to have the same order of magnitude.[59] However, since the Mössbauer and EPR measurements were performed at cryogenic temperatures, information concerning the energies of the excited states are not available from these studies and, therefore, the magnitude of the exchange coupling interactions could not be determined. Early attempts to determine the coupling constant had been made by analysis of the temperature-dependent EPR relaxation behavior[63] and by simulation of the EPR line shape.[64,65] Both of these early studies assumed the presence of an excited state of spin $S = {}^3/_2$. Their analyses suggested that the state is at about 100 cm^{-1}, corresponding to a coupling constant of 40 cm^{-1}. A later magnetic susceptibility measurement performed on the oxidized *D. gigas* Fd II, however, indicated the absence of such a state and set a lower limit of 200 cm^{-1} for J for the oxidized [3Fe-4S] cluster.[40] Consistent with the magnetization measurement, our analysis of the temperature dependent proton NMR isotropic shifts indicates that $J \approx 300$ cm^{-1}. Furthermore, the observed different types of temperature dependent behavior establish that the coupling constants between the iron sites are slightly different: $\Delta J/J = 0.02$. This small, yet measurable, difference is expected since the core structure of the oxidized [3Fe-4S] cluster determined from crystallographic data shows three nearly indistinguishable iron sites.[19] They can be differentiated, however, through the binding cysteine residues.

It has been suggested that the pattern of the contact shifts of the β-CH_2 protons are determined by the orientation of the cysteine ligand with respect to its coordinated Fe site, and the ratio of their contact shifts can be estimated using the following formula (ref 58 and references therein):

$$\frac{\delta_l}{\delta_s} = \frac{[(b_0/b_2) + \cos^2 \phi_l]}{[(b_0/b_2) + \cos^2 \phi_s]} \qquad (8)$$

Here $b_0/b_2 \approx 0.1$ is a constant and the subscripts l and s designate the C_β protons that yield the larger and smaller shifts, respectively. The angles ϕ_l and ϕ_s depends on the dihedral angle, ϕ_α, between the Fe–S–C_β and S–C_β–C_α planes, and the spin delocalization mechanism.[58] For σ-spin delocalization,

$$\phi_l \text{ or } \phi_s = \phi_\alpha + 120° \text{ or } \phi_\alpha - 120° \qquad (9)$$

Table I. Estimated Ratios of Contact Shifts of the C_β Methylene Protons of the Coordinated Cysteine of Oxidized *D. gigas* Fd II

			δ_l/δ_s	
Fe site	coord Cys	ϕ_α[a] (deg)	σ-spin delocalization	π-spin delocalization
1	Cys 8	68.3	2.23	5.93
2	Cys 14	79.5	1.46	2.47
3	Cys 50	92.3	1.09	1.22

[a] Data derived from refs 18 and 19 and from coordinates provided by Dr. L. C. Sieker.

and for π-spin delocalization,

$$\phi_l \text{ or } \phi_s = \phi_\alpha - 30° \text{ or } \phi_\alpha - 150° \qquad (10)$$

Since the unique temperature dependence of the resonances *a* and *b* has provided the means for their unambiguous assignment, and since the crystallographic structure of the oxidized *D. gigas* Fd II has been determined to a 1.7 Å resolution[18,19] (see Figure 1), attempts can be made to identify the cysteine residue responsible for the resonances *a* and *b*. In Table I, the dihedral angles, ϕ_α, for the three cysteine ligands are listed. Using equations (8–10), the ratios of the hyperfine shifts for the three pairs of the β-CH_2 protons are estimated and are also listed in Table I. Assuming a reasonable value of 3.0 ppm for the diamagnetic shift for the C_β methylene protons,[58] the ratio of the observed contact shifts for the peaks *a* and *b* is calculated to be 1.2. Comparison of this observed value with the theoretical data listed in Table I suggests that the resonances *a* and *b* may be attributed to Cys 50, regardless of the spin delocalization mechanism. We would, however, like to comment that such an assignment can only be considered tentative due to the primitive nature of the theory. More definitive or affirmative assignment will have to await detailed isotopically labeled studies.

In our analysis, we have assumed that one of the iron sites, termed iron site 3, is distinguishable from the other two sites based on the exchange coupling interactions. The theoretical prediction of such an assumption is that the C_β methylene proton shifts of the cysteine coordinated to iron site 3 should exhibit Curie type temperature dependence. The fact that only two NMR resonances, *a* and *b*, show Curie type behavior strongly support this assumption. The above assignment for resonances *a* and *b* further suggest that the distinguishable site is the iron site that ligated to the residue Cys 50. Although there is no apparent reason for the iron sites to retain their symmetry upon reduction, it is intriguing to note that the reduced [3Fe-4S] cluster does contain a distinguishable ferric site and the additional electron is shared by the two other iron atoms.[30] Since the temperature dependence of proton NMR shifts contain detailed structural and electronic information about the cluster, as demonstrated in this report, it would be interesting to perform a similar measurement on the reduced *D. gigas* Fd II and to identify the ferric site and the ferric–ferrous pair. Research along this line of investigation is currently underway in our laboratories and the preliminary results are promising.

Acknowledgment. We thank Dr. L. C. Sieker for providing us the X-ray crystallographic coordinates of *D. gigas* Fd II. This work is supported by the National Institutes of Health Grants GM 41482 (J.L.G. and J.J.G.M.) and GM 32187 (B.H.H.), the National Science Foundation Grant DMB 9001530 (B.H.H.), and grants (I.M. and J.J.G.M.) from the Instituto Nacional de Investigação Cientifica and from the Junta National de Investigação Cientifica e Tecnológica. This research is also supported in part by the University Research Committee of Emory University and by a Biomedical Research Support Grant (B.H.H.) from the National Center for Research Resources.

(63) Gayda, J.-P.; Bertrand, P.; Theodule, F.-X.; Moura, J. J. G. *J. Chem. Phys.* **1982**, *77*, 3387–3391.
(64) Guigliarelli, B; Gayda, J. P.; Bertrand, P.; More, C. *Biochim. Biophys. Acta* **1986**, *871*, 149–155.
(65) Guigliarelli, B.; More, C.; Bertrand, P.; Gayda, J. P. *J. Chem. Phys.* **1986**, *85*, 2774–2778.